Supplementary Information

Ring-closing metathesis of dialkenyldisilacycloalkanes for the synthesis of disilabicycloalkanes and tetrasilatricycloalkanes

Yuyang Tu,[a] Yusuke Inagaki,[a] Kazuaki Ohara,[b] Kentaro Yamaguchi,[b] and Wataru Setaka*,[a]

[a] *Division of Applied Chemistry, Faculty of Urban Environmental Sciences, Tokyo Metropolitan University, 1-1 Minami-Osawa, Hachioji, Tokyo 192-0397, Japan.*

[b] *Faculty of Pharmaceutical Sciences at Kagawa Campus, Tokushima Bunri University, 1314-1 Shido, Sanuki, Kagawa 769-2193, Japan.*

Table of Contents:

1. Synthetic Details

a. Figures

(a) (b)

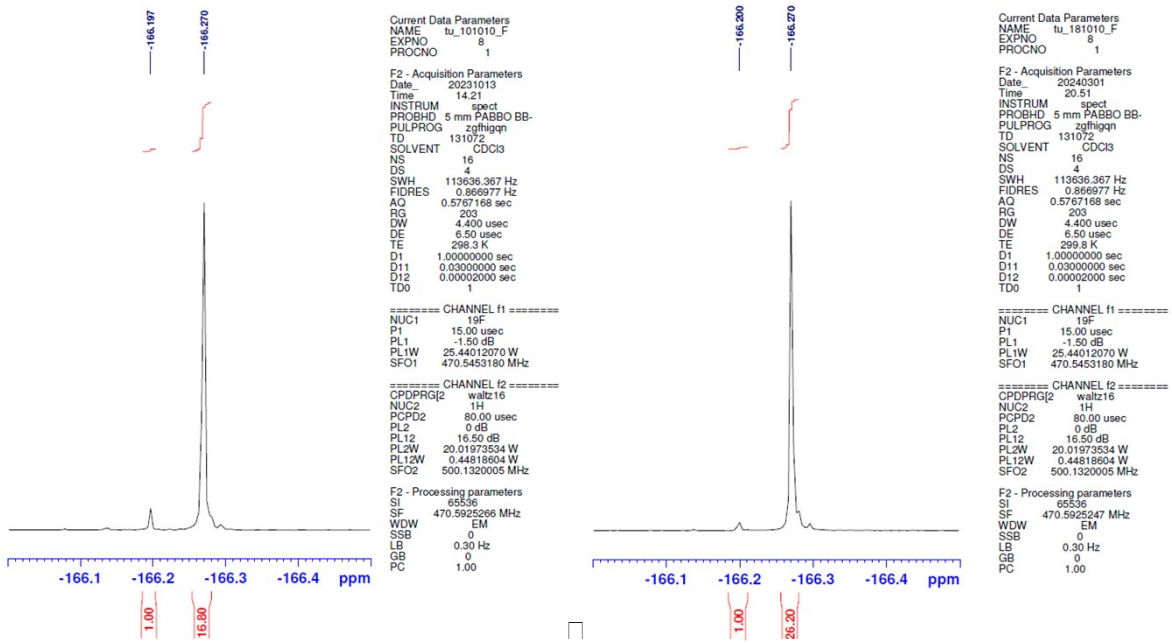

Fig. S1. ^{19}F NMR spectra of the precursor **3** (The signals at −166.20 and −166.27 are assignable to cis-**3** and trans-**3**, respectively.): (a) for the synthesis of bicyclo[10.10.10]alkanes (Entry 1 in Table 1); (b) for the synthesis of bicyclo[18.10.10]alkanes (Entry 2 in Table 1).

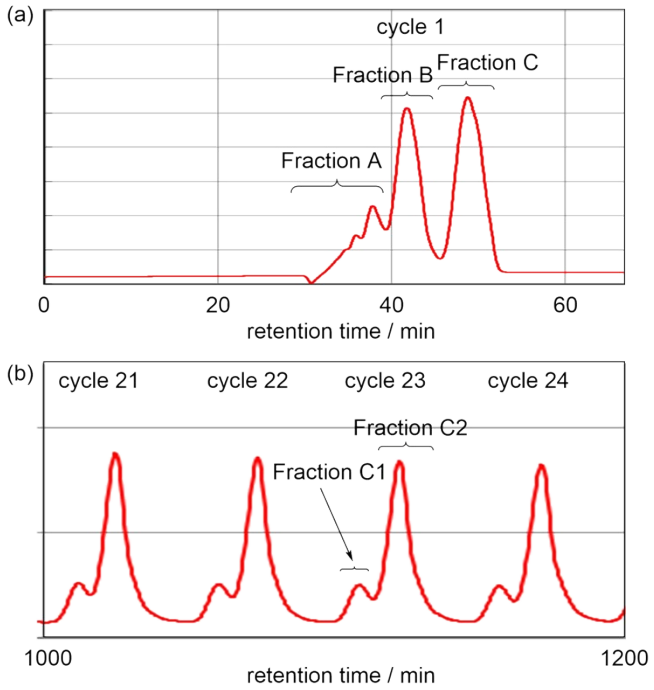

Fig. S2. Recycling GPC charts (RI-detector) of the crude product mixture in the synthesis of bicyclo[18.10.10]alkane (Entry 2 in Table 1).

b. General and Materials

General All NMR spectra in solution were recorded using a Bruker AVANCEIII 500 spectrometer. Chemical shifts in the ^{1}H and ^{13}C NMR spectra were based on residual solvent resonances, whereas those in ^{29}Si NMR spectra were referenced to external tetramethylsilane. High-resolution mass spectrometry (HRMS) analyses were performed with Fourier transform ion cyclotron resonance mass spectrometry using SolariX 9.4 T (Bruker Daltonics). Mass spectra were calibrated using external calibration with tuning-mix (Agilent, Santa Clara, CA, US). The instrument parameters for APCI mode were as follows: the sample flow rate was 2 μL /min, the desolvation plate temperature was 220 °C, the rate of N_2 drying gas was 3.0-3.5 L/min, the rate of N_2 nebulizing gas was 1.5-2.0 L/min, APCI probe heater was 370 °C, the corona discharge needle was 0.5 – 1.0 kV and the capillary voltage was 4.5 kV for the positive ion detection mode.

Materials Commercially available reagents were used as received without further purification.

c. Synthesis of 4

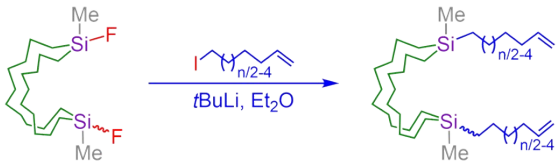

cis/trans-**3**[S1]

4a; n = 10
4b; n = 18

Synthesis of 4a *t*-BuLi (1.7 M in pentane, 10.1 mL, 17.1 mmol) was added to a dry Et_2O (30 mL) solution of **3**[S1] (1.50 g, 3.71 mmol) and 6-iodohex-1-ene (1.71 g, 8.16 mmol) at –78 °C and the resulting solution was stirred at –78 °C for 30 min and at room temperature for 12 h. The reaction was quenched with NH_4Cl aq. and extracted with hexane. The organic layer was dried over Na_2SO_4, concentrated, and purified by silica gel column chromatography (hexane), which furnished **4a** (1.81 g, 3.51 mmol, 90% yield) as a colorless oil.

4a: a colorless oil; ^{1}H NMR ($CDCl_3$, 500 MHz, 7.24 ppm): δ 5.79 (ddt, J = 17, 10, 7.2 Hz, 2H, H_2C=C*H*-), 4.97 (d, J = 17 Hz, 2H, *H*$_2$C=CH-), 4.92 (d, J = 10 Hz, 2H, *H*$_2$C=CH-), 2.04 (q, J = 7.2 Hz, 4H, H_2C=CH-C*H*$_2$), 1.43-1.20 (br, 40H), 0.55-0.43 (br, 12H, -Si-C*H*$_2$-), −0.11 (s, 6H, C*H*$_3$-Si); $^{13}C\{^{1}H\}$ NMR ($CDCl_3$, 126 MHz, 77 ppm): δ 139.2, 114.0, 33.5, 33.0, 33.0, 29.1, 28.7, 23.4, 23.4, 14.0, 13.2, −4.9; $^{29}Si\{^{1}H\}$ NMR ($CDCl_3$, 99 MHz): δ 3.1. HRMS (APCI) *m/z*: $[M\text{-}CH_3\text{+}H_2O]^+$ Calcd for $C_{33}H_{67}OSi_2$ 535.47250; Found: 535.47182.

Synthesis of 4b The title compounds pure **4b** (1.52 g, 2.36 mmol, 92% isolated yield) was obtained from **3** (1.03 g, 2.56 mmol) and 10-iodo-1-decene (1.50 g, 5.62 mmol) in dry Et_2O (20 mL) by the same procedure as that for synthesis of **4a**.

4b: a colorless oil; ^{1}H NMR ($CDCl_3$, 500 MHz, 7.24 ppm): δ 5.80 (ddt, J = 17, 10, 7.9 Hz, 2H, H_2C=C*H*-), 4.97 (d, J = 17 Hz, 2H, *H*$_2$C=CH-), 4.91 (d, J = 10 Hz, 2H, *H*$_2$C=CH-), 2.02 (q, J = 7.9 Hz, 4H, H_2C=CH-C*H*$_2$), 1.40-1.18 (br, 56H), 0.52-0.40 (br, 12H, -Si-C*H*$_2$-), −0.11 (s, 6H, C*H*$_3$-Si); $^{13}C\{^{1}H\}$ NMR ($CDCl_3$, 126 MHz, 77 ppm): δ 139.3, 114.1, 33.8, 33.8, 33.0, 29.4, 29.3, 29.2, 29.1, 28.9, 28.7, 23.9, 23.4, 14.1, 13.2, −4.9; $^{29}Si\{^{1}H\}$ NMR ($CDCl_3$, 99 MHz): δ 3.0. HRMS (APCI) *m/z*: $[M\text{-}CHCH_2\text{+}H_2O]^+$ Calcd for $C_{40}H_{83}OSi_2$ 635.59770; Found: 635.59534.

d. RCM reactions of 4

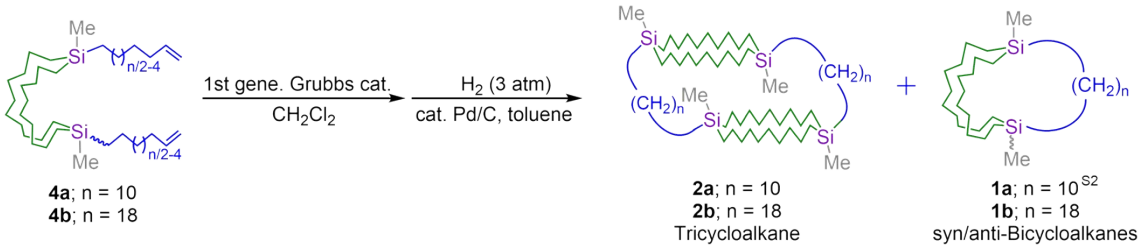

4a; n = 10
4b; n = 18

2a; n = 10
2b; n = 18
Tricycloalkane

1a; n = 10 [S2]
1b; n = 18
syn/anti-Bicycloalkanes

RCM reaction of 4a To a 1000-mL three-necked flask with a magnetic stirrer, condenser, and glass stoppers, **4a** (0.69 g, 1.29 mmol) and dry CH_2Cl_2 (520 mL) was added. Then, 1st generation Grubbs catalyst (0.12 g, 0.14 mmol) was added to the flask, and the solution was stirred under reflux for 16h. After confirming the completeness of the reaction by ^{1}H NMR, the reaction mixture was cooled to room temperature, and the solvent was removed under reduced pressure. The residue was treated with column chromatography (silica gel, eluent: hexane) to remove metal complexes.

Without further purification, the mixture of crude products (0.61 g), toluene (15 mL), and Pd/C catalyst (ca. 50 mg) were added to an autoclave. The vessel was heated to 75 °C and stirred for 12 h under a hydrogen atmosphere (3 atm). The reaction mixture was filtered, and volatile materials were removed in vacuo. The desired **2a** (197 mg, 0.19 mmol, 30% yield), **syn-1a** [S2] (11 mg, 0.02 mmol, 1.7% yield), and **anti-1a** [S2] (56 mg, 0.11 mmol, 8.6% yield) was separated by gel permeation chromatography.

2a: colorless crystals; mp 48.9-51.7 °C; ^{1}H NMR ($CDCl_3$, 500 MHz, 7.24 ppm): δ 1.32-1.22 (br, 108H), 0.54-0.40 (br, 24H, -Si-C*H*2-), −0.10 (s, 12H, CH_3-Si). ^{13}C{^{1}H} NMR ($CDCl_3$, 126 MHz, 77 ppm): δ 33.1, 33.0, 29.0, 28.9, 28.8, 28.7, 23.6, 23.4, 13.9, 13.3, −4.7; ^{29}Si{^{1}H} NMR ($CDCl_3$, 99 MHz): δ 3.2; HRMS (APCI) *m/z*: $[M\text{-}CH_3\text{+}H_2O]^+$ Calcd for $C_{63}H_{131}OSi_4$ 1015.92715; Found: 1015.92661.

RCM reaction of 4b The desired compounds **2b** (117 mg, 0.09 mmol, 8.0% yield), **syn-1b** (72 mg, 0.12 mmol, 5.0% yield), and **anti-1b** (339 mg, 0.55 mmol, 23% yield) were obtained from **4b** (1.52 g, 2.36 mmol) in CH_2Cl_2 (950 mL) by the same procedure as that for RCM of **4a**.

2b: colorless crystals; mp 65.8-66.2 °C; ^{1}H NMR ($CDCl_3$, 500 MHz, 7.24 ppm): δ 1.40-1.10 (br, 128H), 0.53-0.41 (br, 24H, -Si-C*H*2-), −0.11 (s, 12H, CH_3-Si). ^{13}C{^{1}H} NMR ($CDCl_3$, 126 MHz, 77 ppm): δ 33.5, 33.0, 29.5, 29.5, 29.4, 29.3, 29.1, 28.7, 23.7, 23.4, 14.0, 13.2, −4.8; ^{29}Si{^{1}H} NMR ($CDCl_3$, 99 MHz): δ 3.1; HRMS (APCI) *m/z*: $[M\text{-}CH_3\text{+}H_2O]^+$ Calcd for $C_{33}H_{67}OSi_2$ 1240.17755; Found: 1240.17324.

syn-1b: a colorless oil; ^{1}H NMR ($CDCl_3$, 500 MHz, 7.24 ppm): δ 1.40-1.20 (br, 64H), 0.58-0.40 (br, 12H, -Si-C*H*2-), −0.13 (s, 6H, CH_3-Si). ^{13}C{^{1}H} NMR ($CDCl_3$, 126 MHz, 77 ppm): δ 33.4, 33.1, 29.4, 29.3, 29.2, 29.1, 29.1, 28.8, 28.6, 23.6, 23.4, 14.2, 13.3, −4.7; ^{29}Si{^{1}H} NMR ($CDCl_3$, 99 MHz): δ 2.9; HRMS (APCI) *m/z*: $[M\text{-}CH_3\text{+}H_2O]^+$ Calcd for $C_{33}H_{67}OSi_2$ 619.; Found: 535.47182.

anti-1b: a colorless oil; ^{1}H NMR ($CDCl_3$, 500 MHz, 7.24 ppm): δ 1.45-1.10 (br, 64H), 0.55-0.42 (br, 12H, -Si-C*H*2-), −0.08 (s, 6H, CH_3-Si). ^{13}C{^{1}H} NMR ($CDCl_3$, 126 MHz, 77 ppm): δ 32.6, 32.3, 29.3, 29.2, 29.2, 29.1, 28.6, 28.6, 28.0, 28.0, 23.4, 23.2, 13.6, 13.4, −4.5; ^{29}Si{^{1}H} NMR ($CDCl_3$, 99 MHz): δ 3.4; HRMS (APCI) *m/z*: $[M\text{-}2xCH_3\text{+}H\text{+}H_2O]^+$ Calcd for $C_{33}H_{67}OSi_2$ 605.55075; Found: 605.54821.

e. References

(S1) Y. Tu, Y. Inagaki and W. Setaka, *J. Org. Chem.*, 2024, **89**, 6222–6229.
(S2) W. Setaka, Y. Ikeda, Y. Inagaki, K. Ohara and K. Yamaguchi, *Org. Lett.* 2023, **25**, 7283–7286.

2. Copies of NMR and HRMS Spectra for All New Compounds

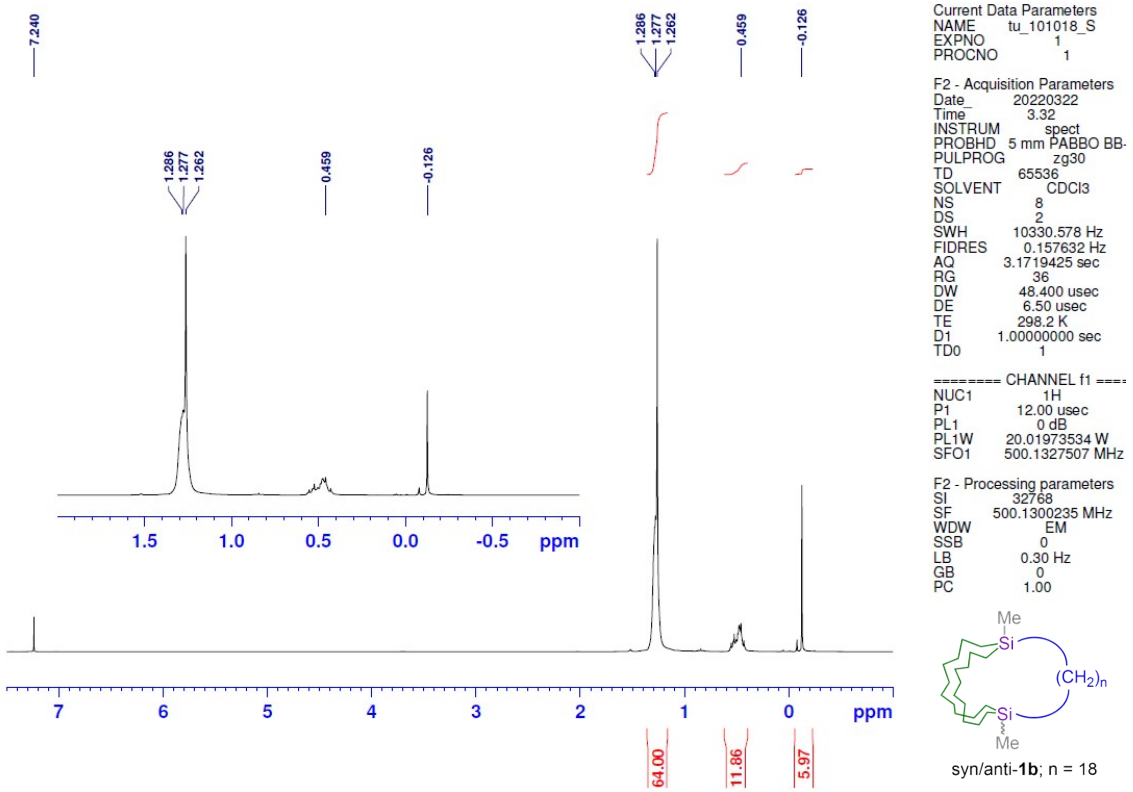

Fig. S3. ^{1}H NMR spectrum of syn-**1b** in $CDCl_3$.

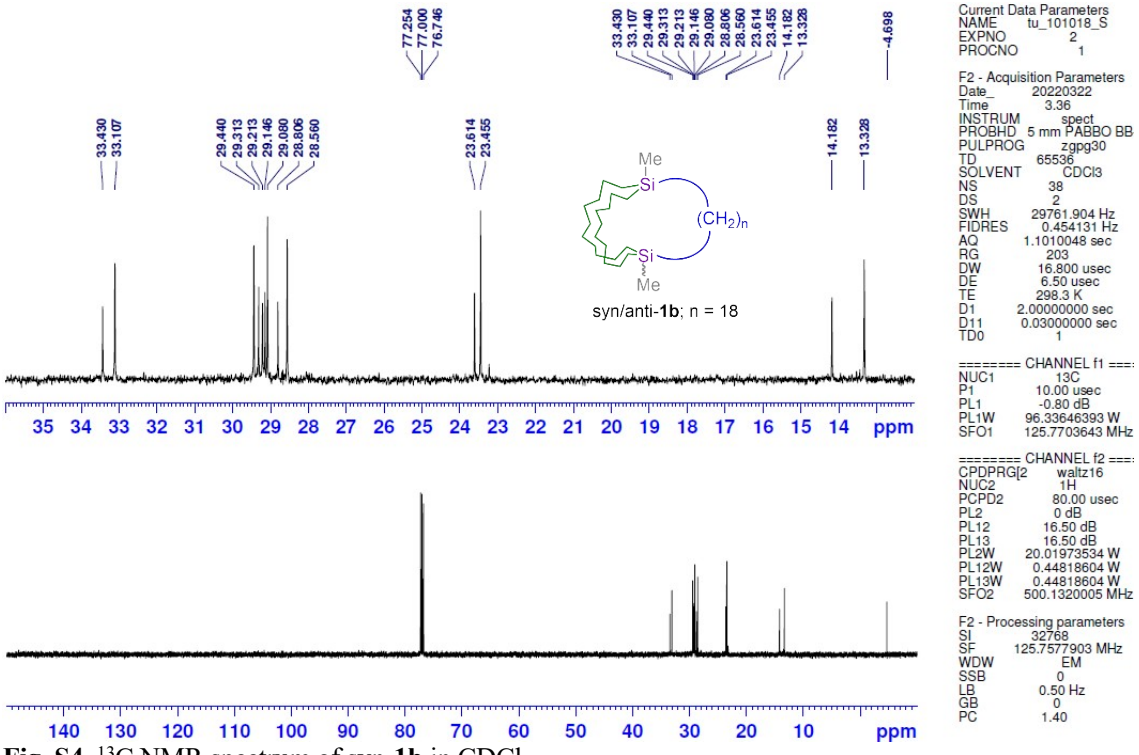

Fig. S4. ^{13}C NMR spectrum of syn-**1b** in $CDCl_3$.

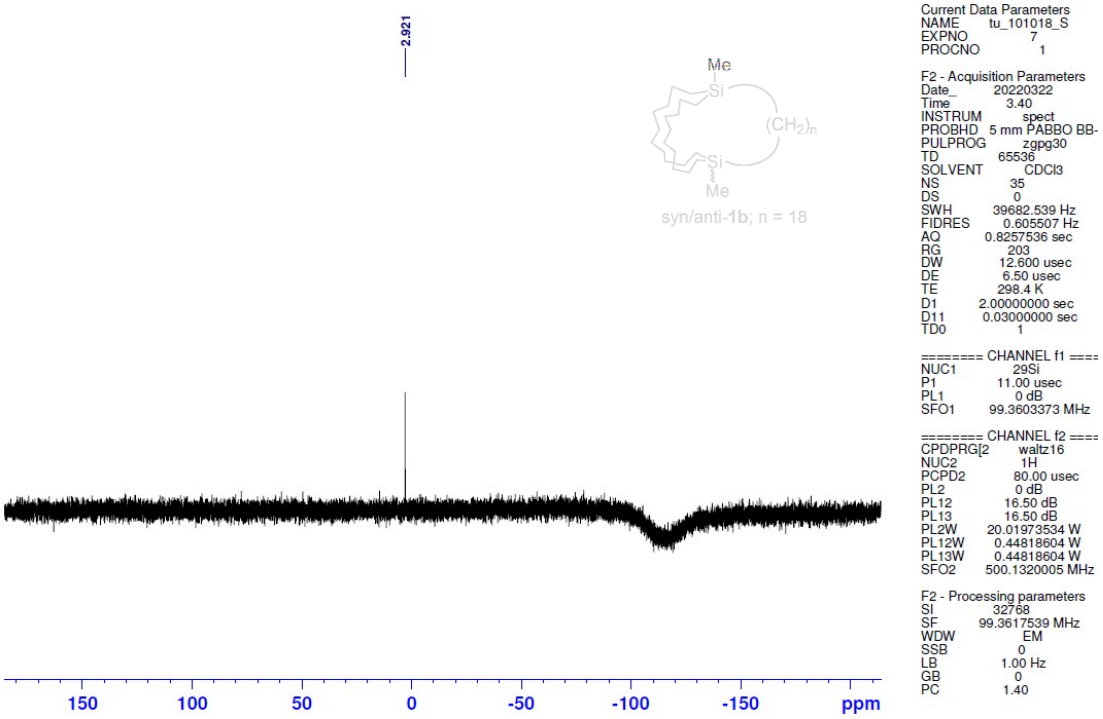

Fig. S5. ^{29}Si NMR spectrum of syn-**1b** in $CDCl_3$.

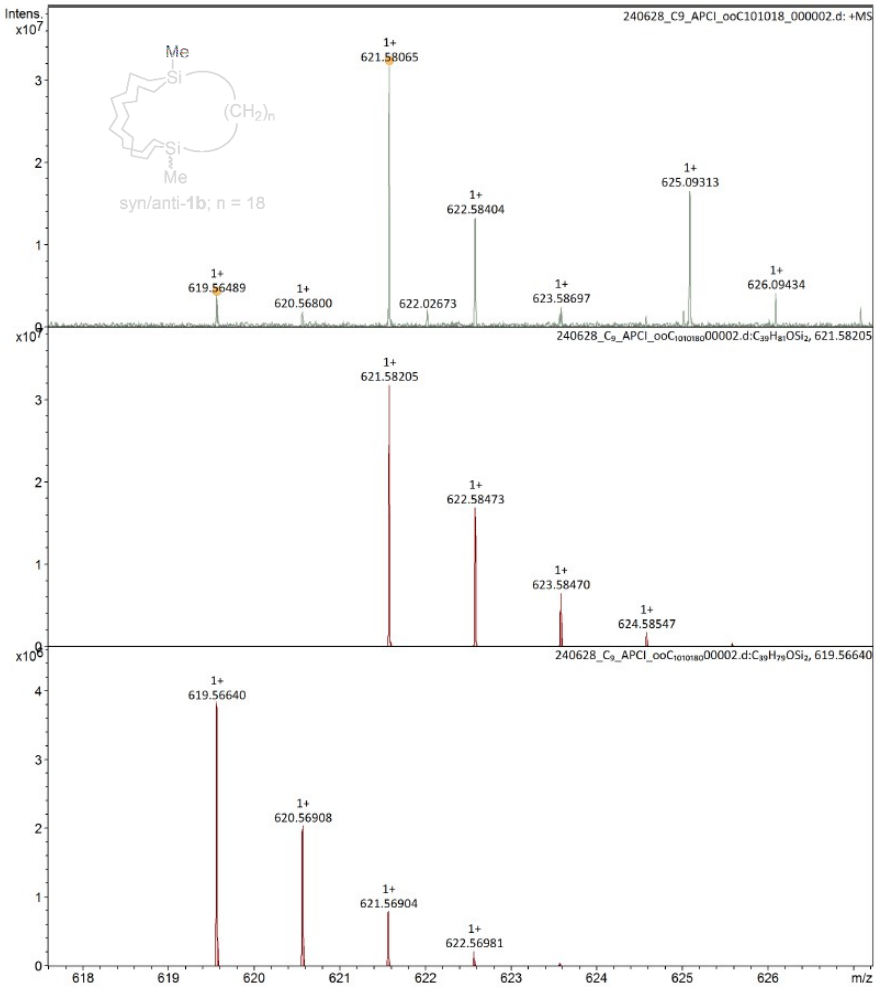

Fig. S6. HRMS spectrum of syn-**1b** (APCI, positive). Top: obsd. Center and Bottom: sim.

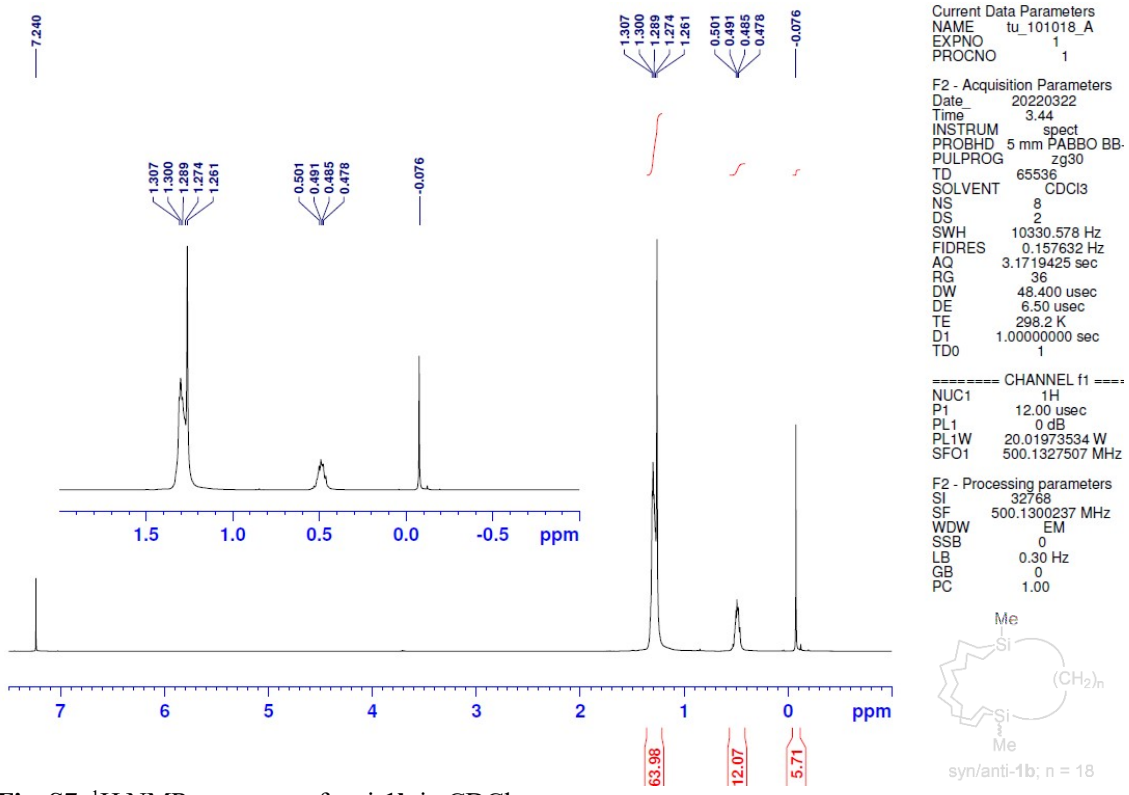

Fig. S7. ^{1}H NMR spectrum of anti-**1b** in $CDCl_3$.

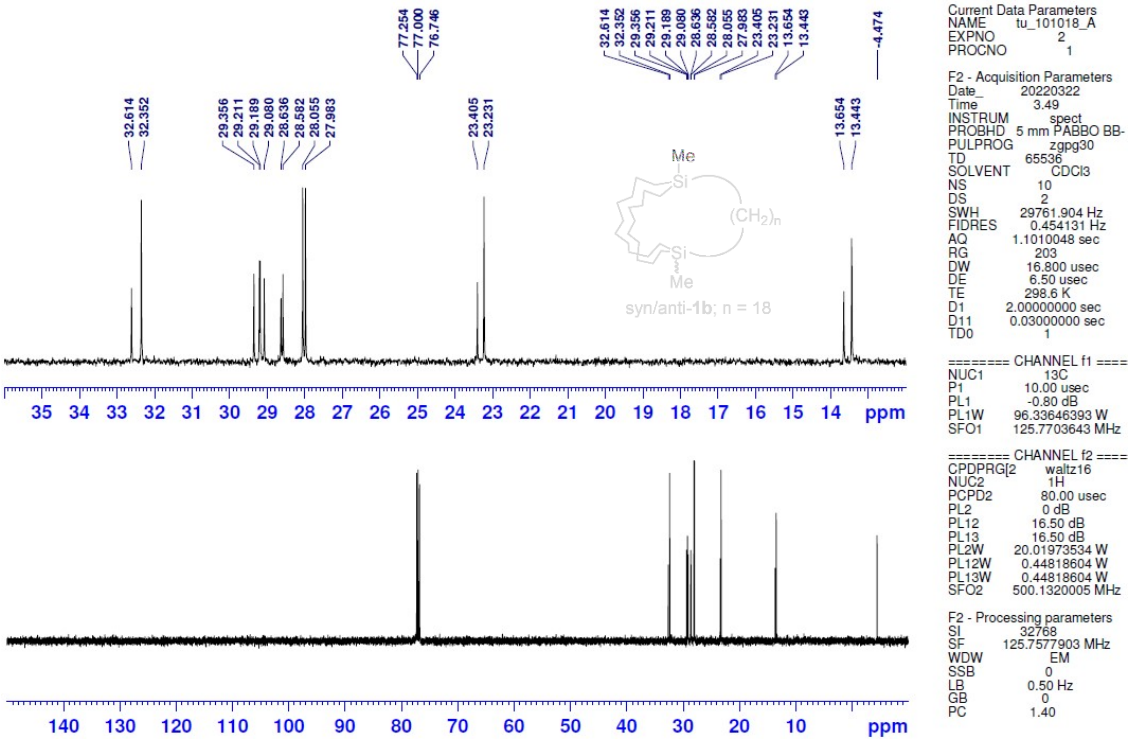

Fig. S8. ^{13}C NMR spectrum of anti-**1b** in $CDCl_3$.

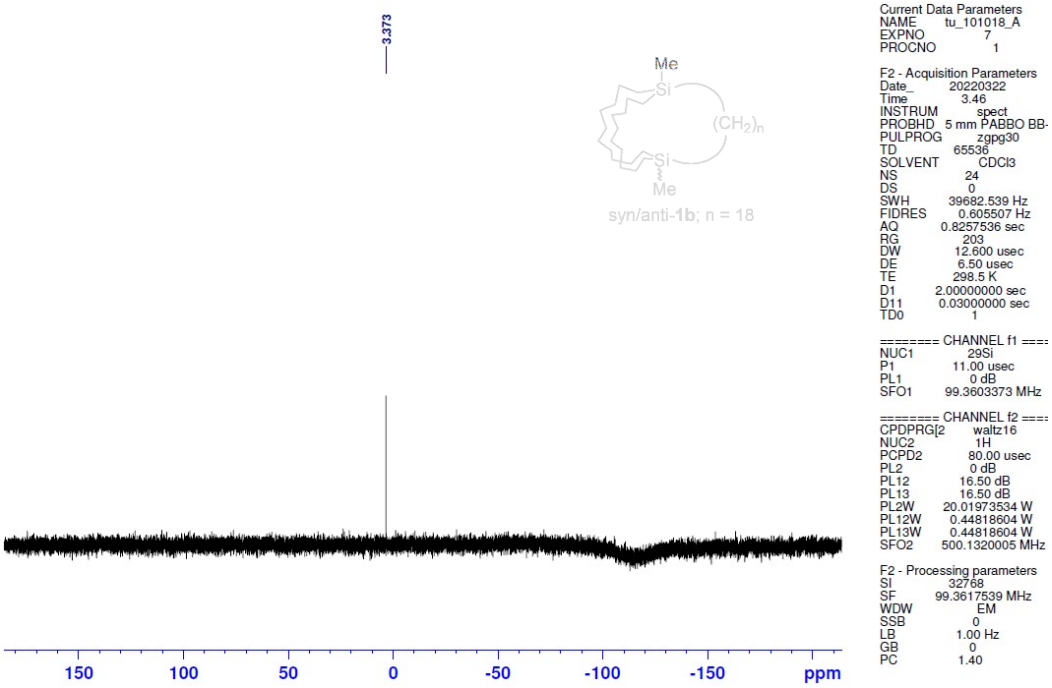

Fig. S9. ^{29}Si NMR spectrum of anti-**1b** in $CDCl_3$.

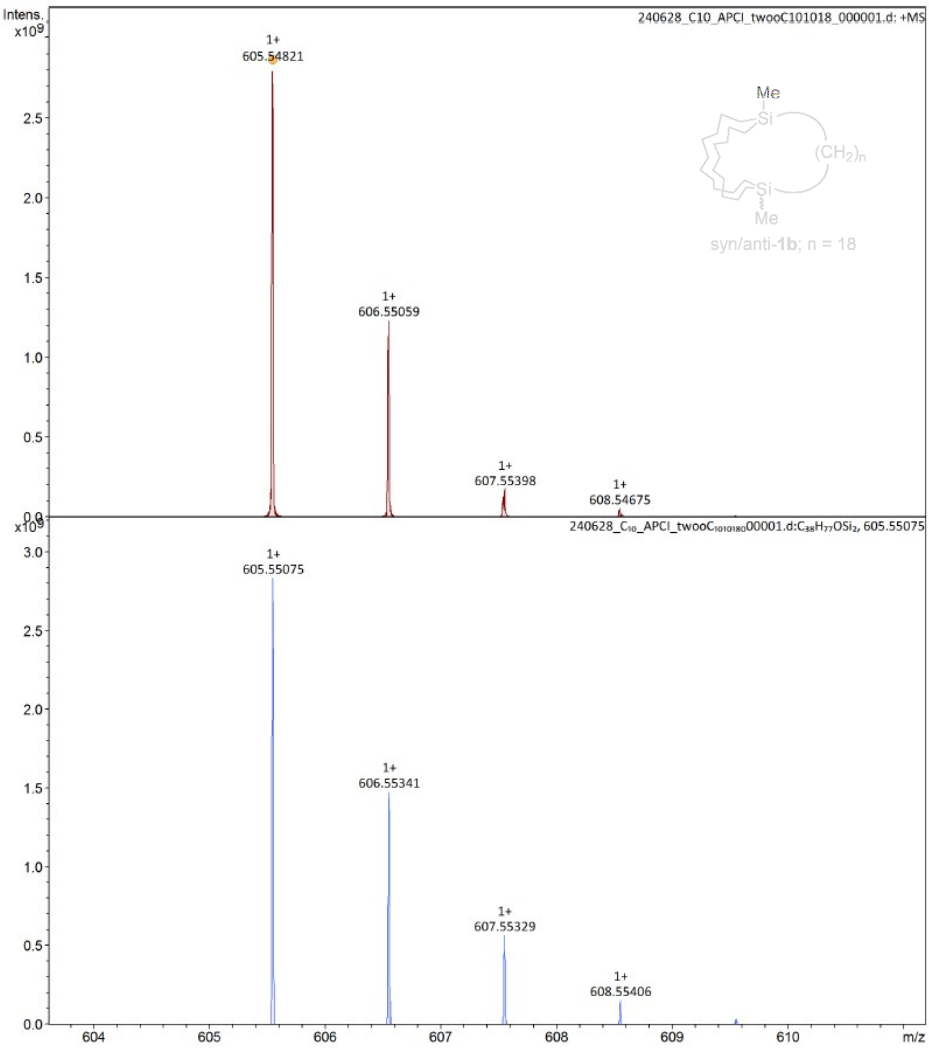

Fig. S10. HRMS spectrum of anti-**1b** (APCI, positive). Top: obsd. Bottom: sim.

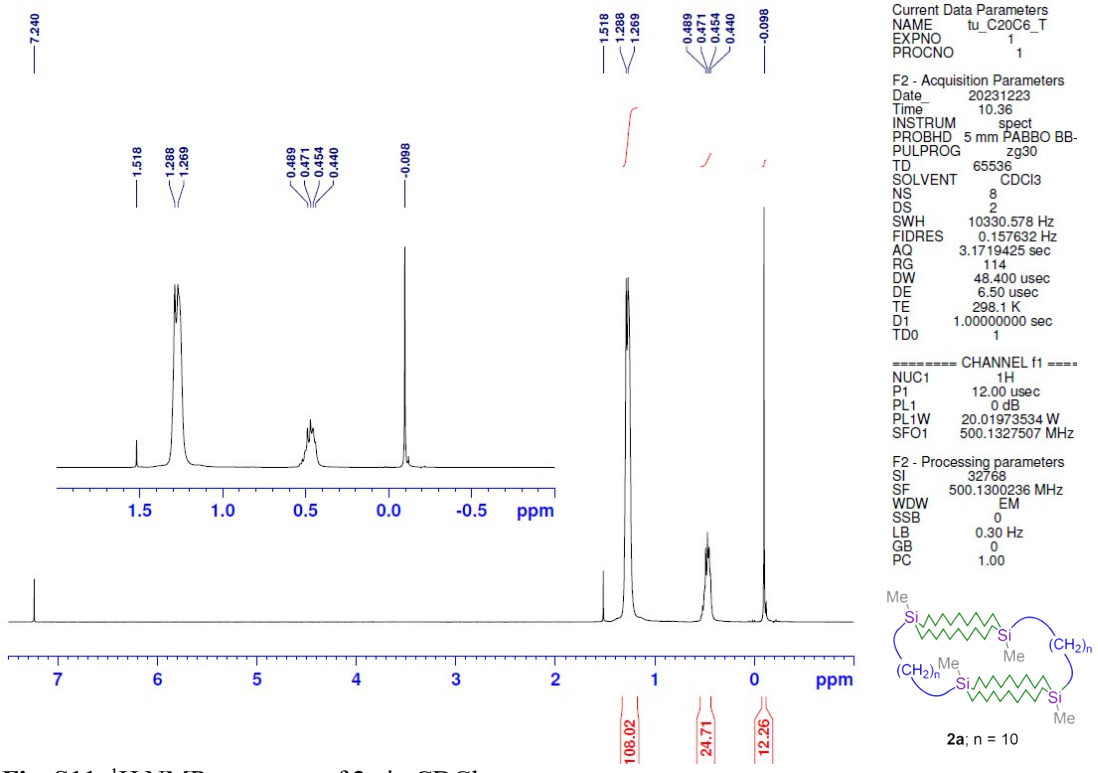

Fig. S11. ^{1}H NMR spectrum of **2a** in $CDCl_3$.

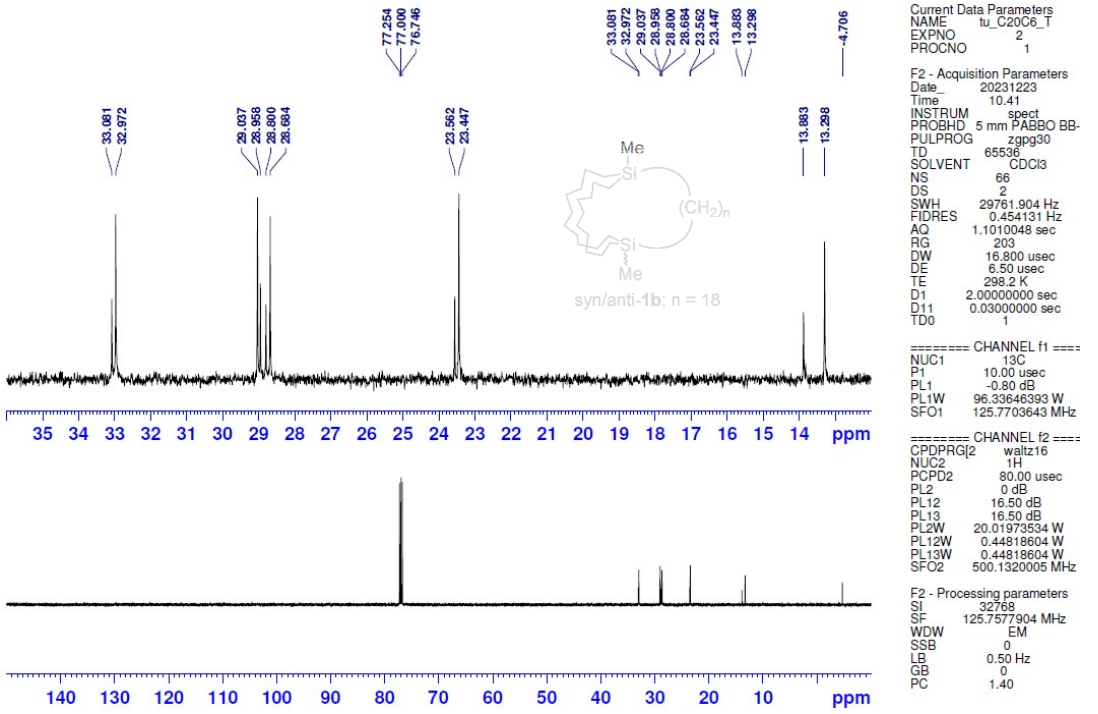

Fig. S12. ^{13}C NMR spectrum of **2a** in $CDCl_3$.

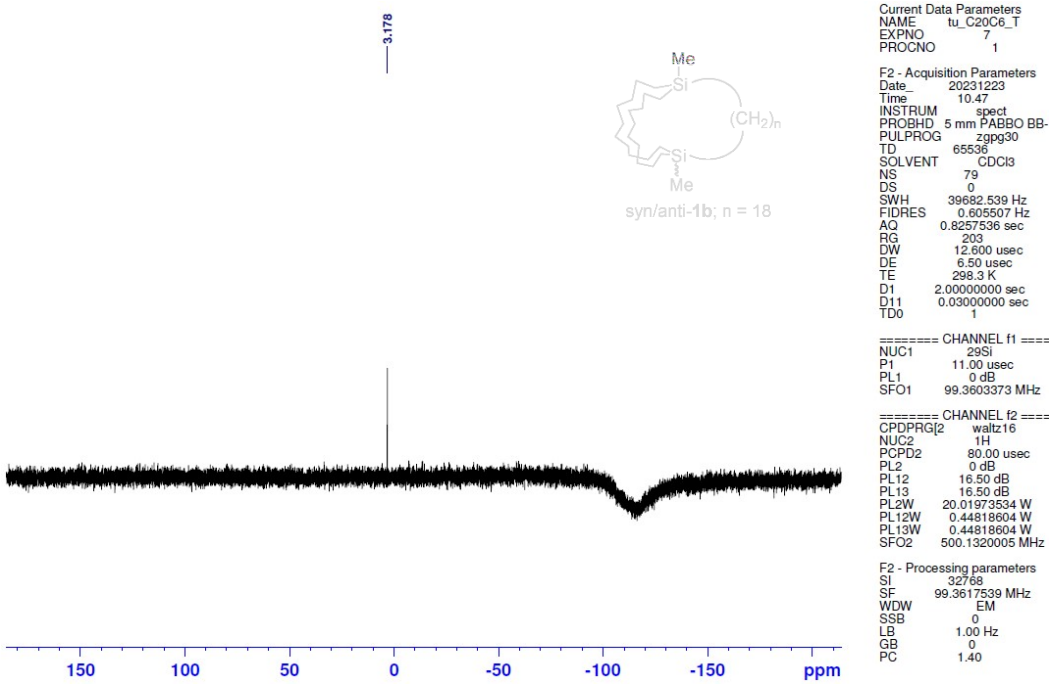

Fig. S13. ^{29}Si NMR spectrum of **2a** in $CDCl_3$.

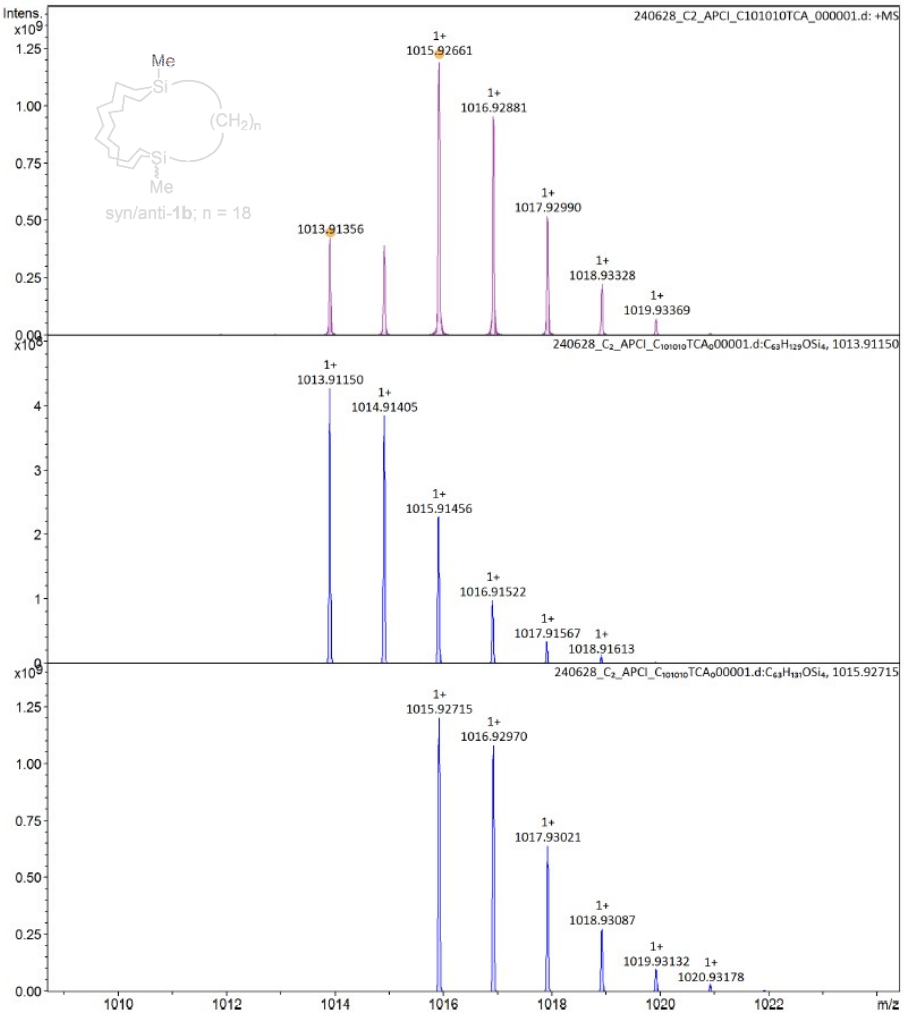

Fig. S14. HRMS spectrum of **2a** (APCI, positive). Top: obsd. Center and Bottom: sim.

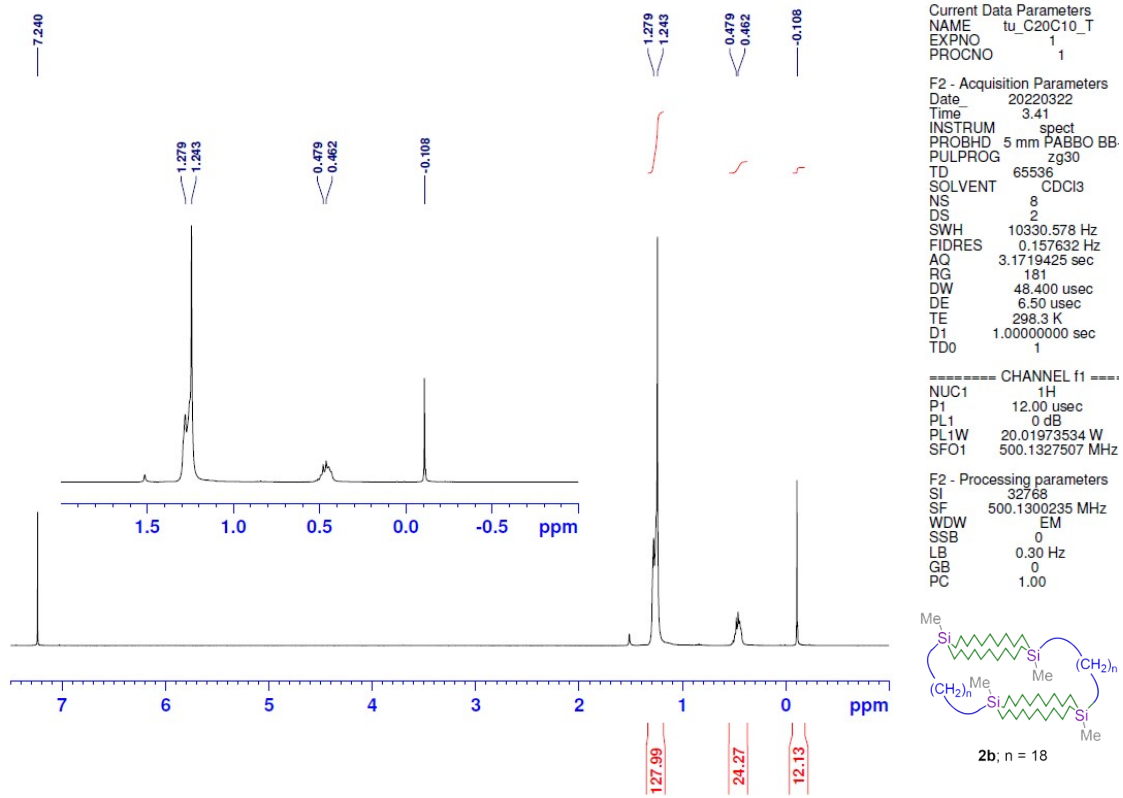

Fig. S15. ^{1}H NMR spectrum of **2b** in $CDCl_3$.

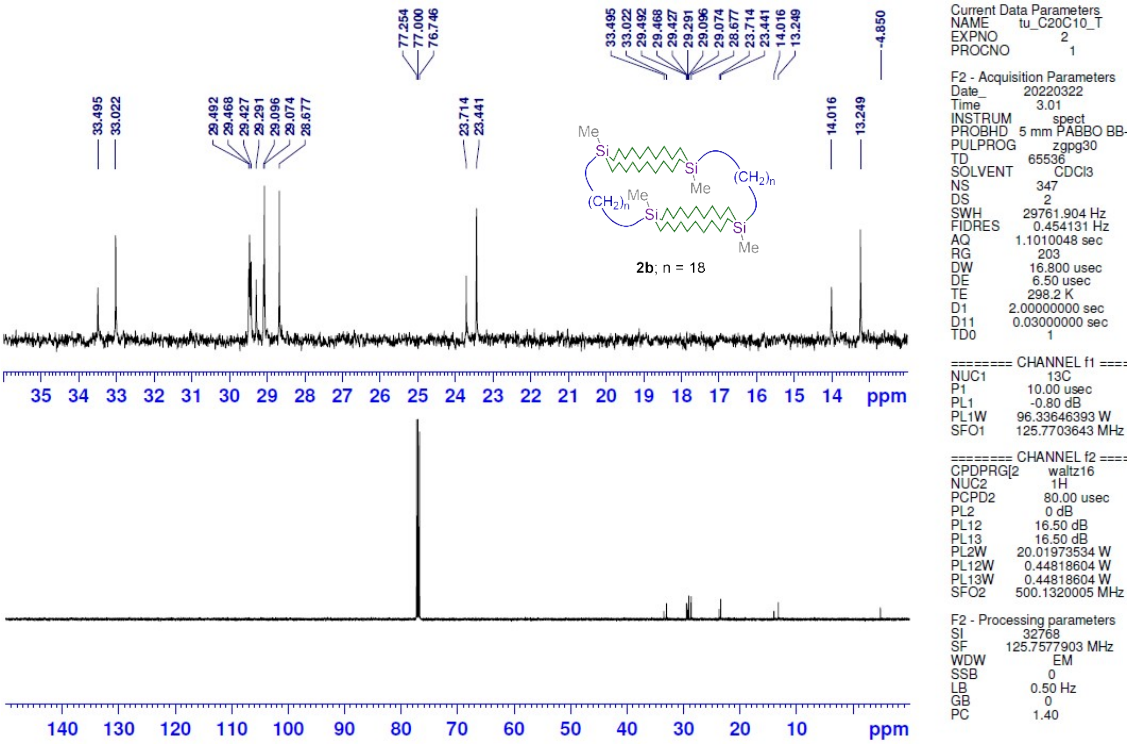

Fig. S16. ^{13}C NMR spectrum of **2b** in $CDCl_3$.

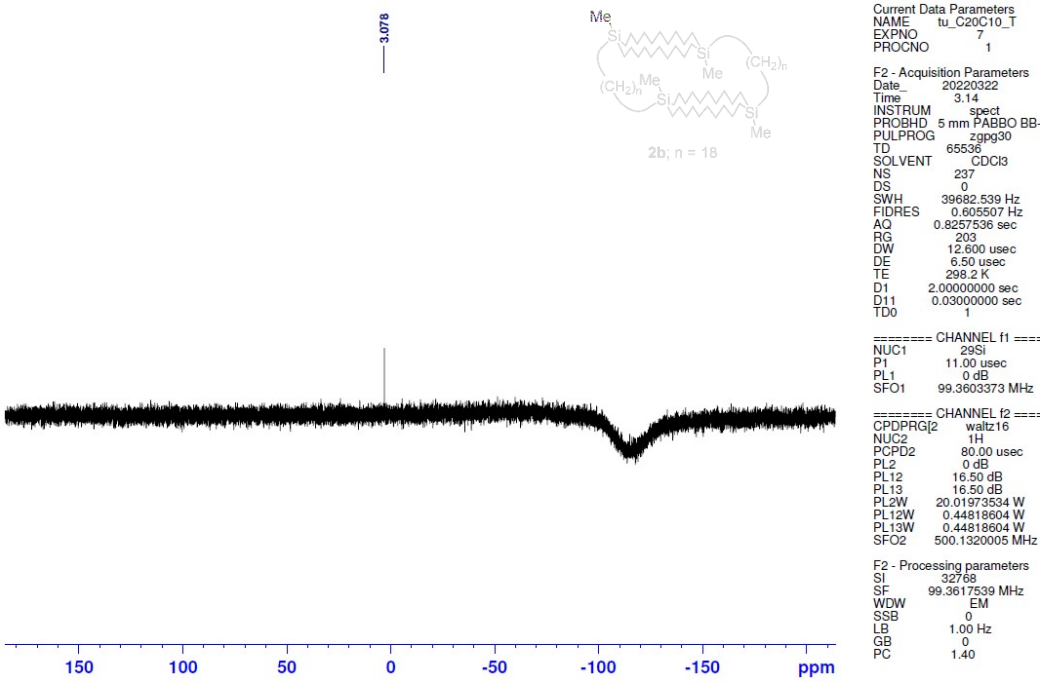

Fig. S17. ^{29}Si NMR spectrum of **2b** in $CDCl_3$.

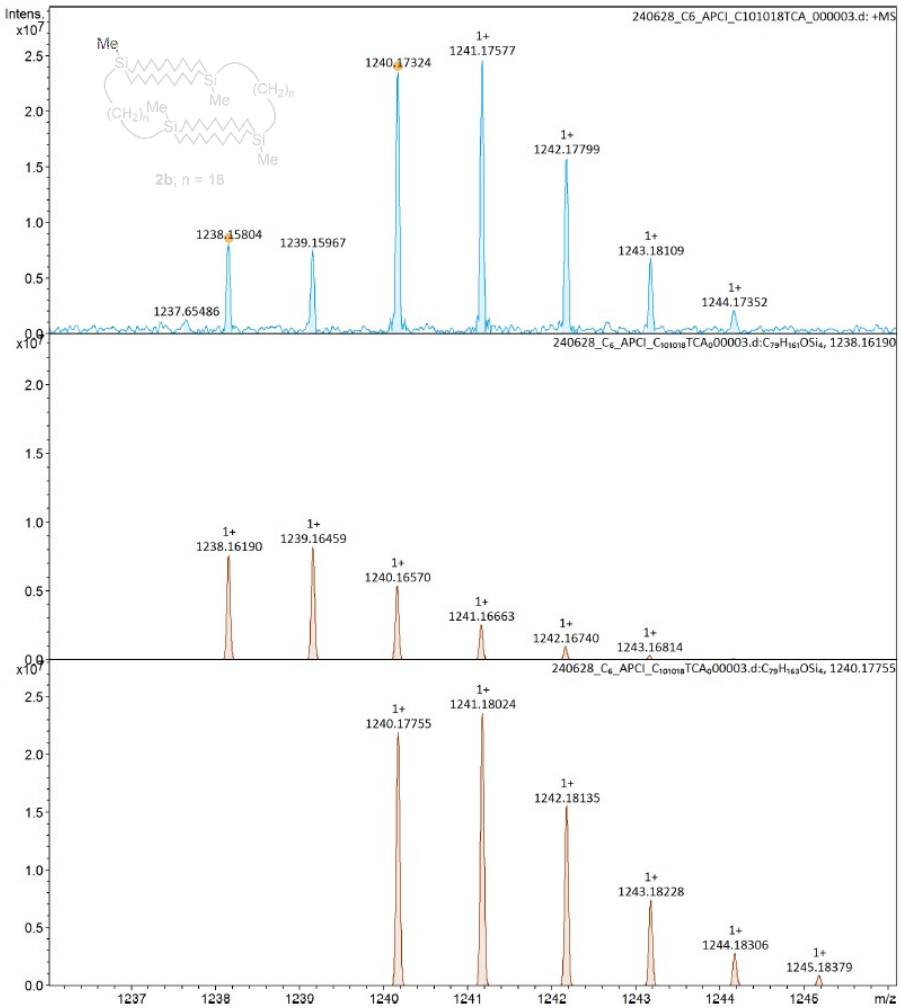

Fig. S18. HRMS spectrum of **2b** (APCI, positive). Top: obsd. Center and Bottom: sim.

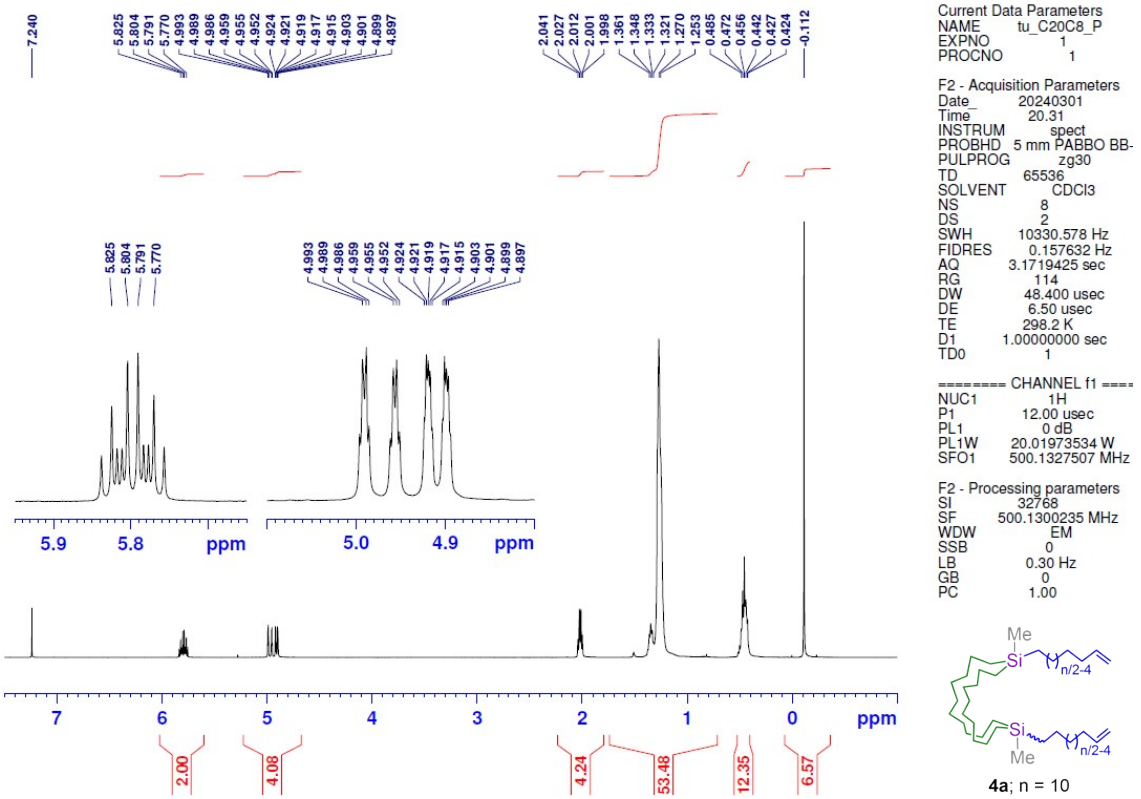

Fig. S19. ^{1}H NMR spectrum of **4a** in $CDCl_3$.

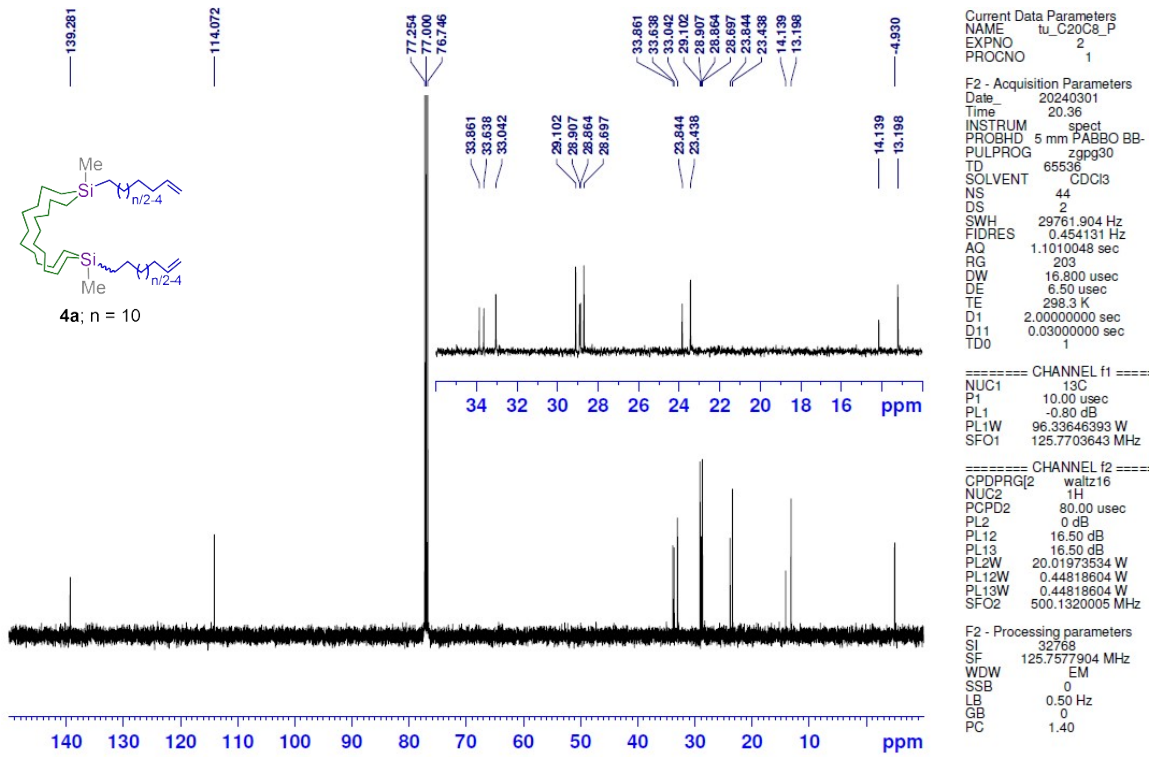

Fig. S20. ^{13}C NMR spectrum of **4a** in $CDCl_3$.

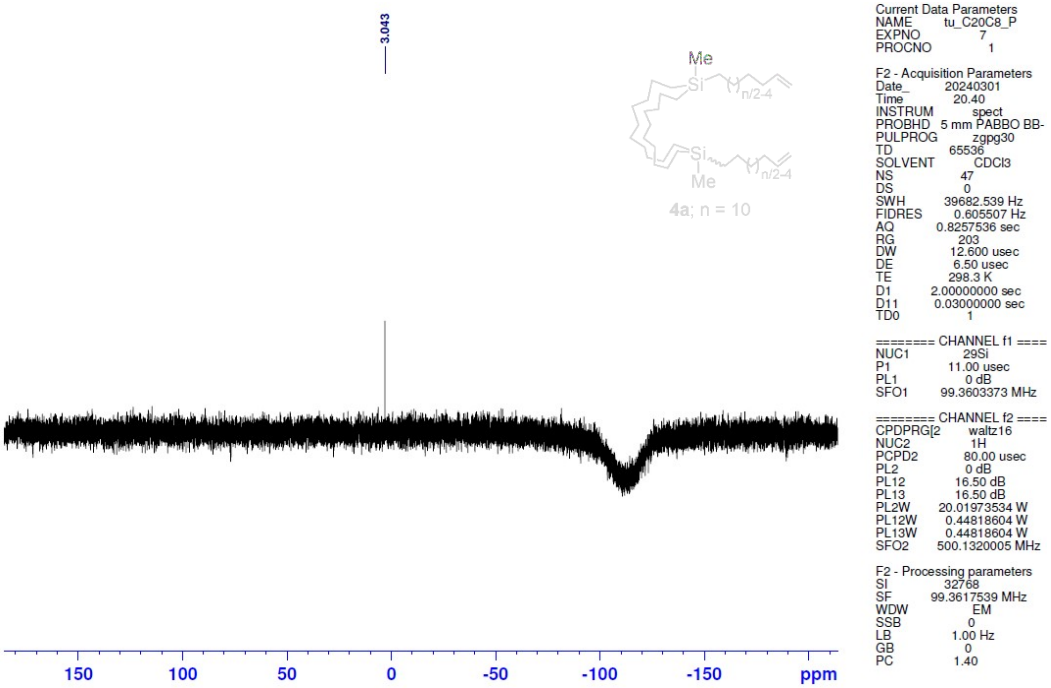

Fig. S21. ^{29}Si NMR spectrum of **4a** in $CDCl_3$.

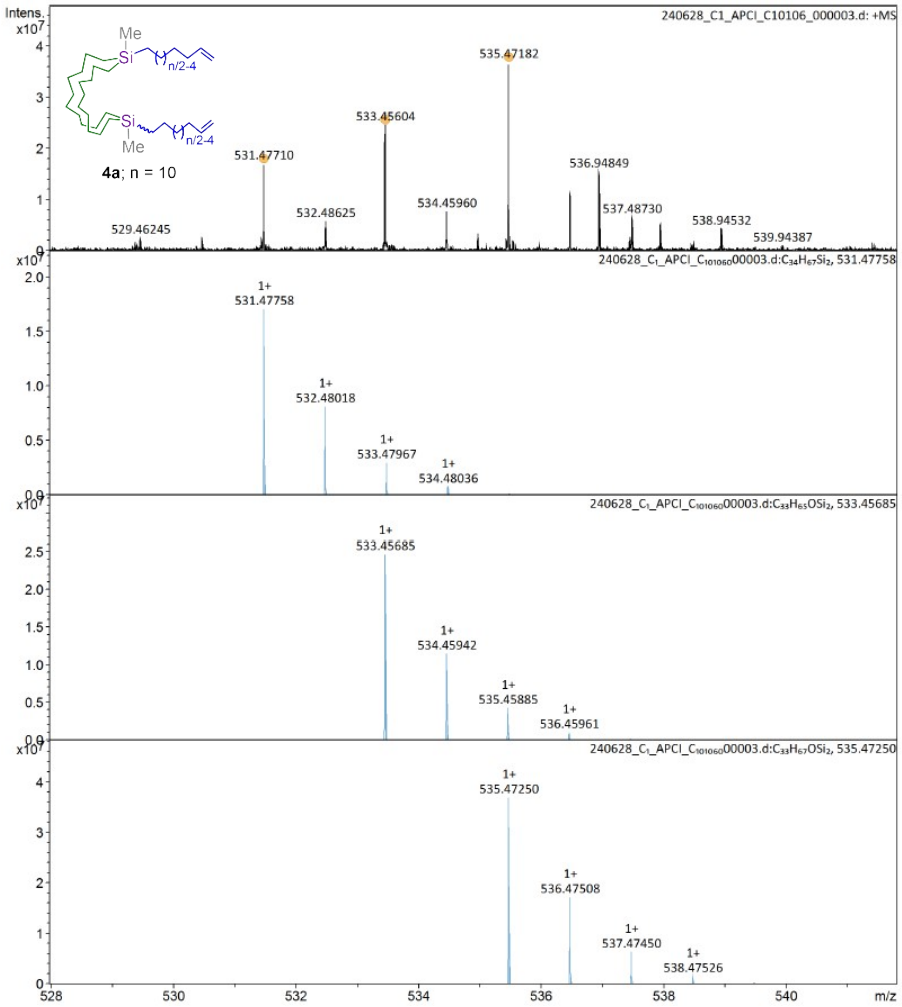

Fig. S22. HRMS spectrum of **4a** (APCI, positive). Top: obsd. Center and Bottom: sim.

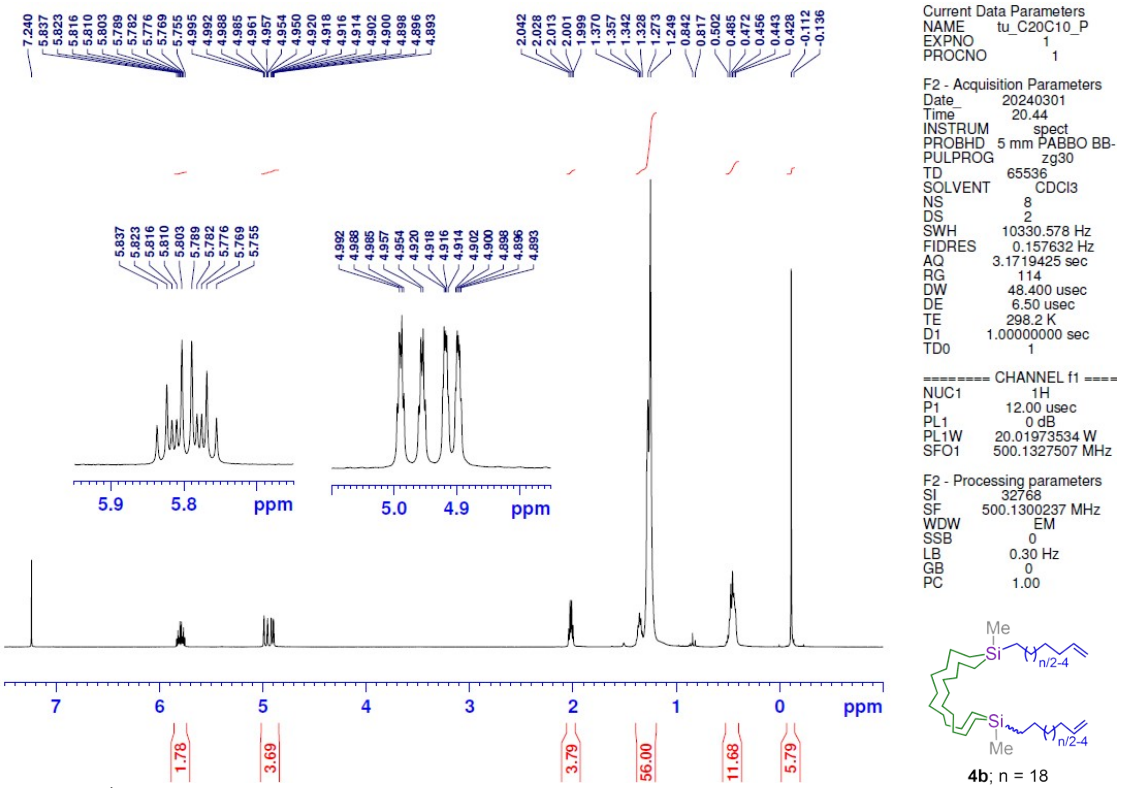

Fig. S23. ^{1}H NMR spectrum of **4b** in $CDCl_3$.

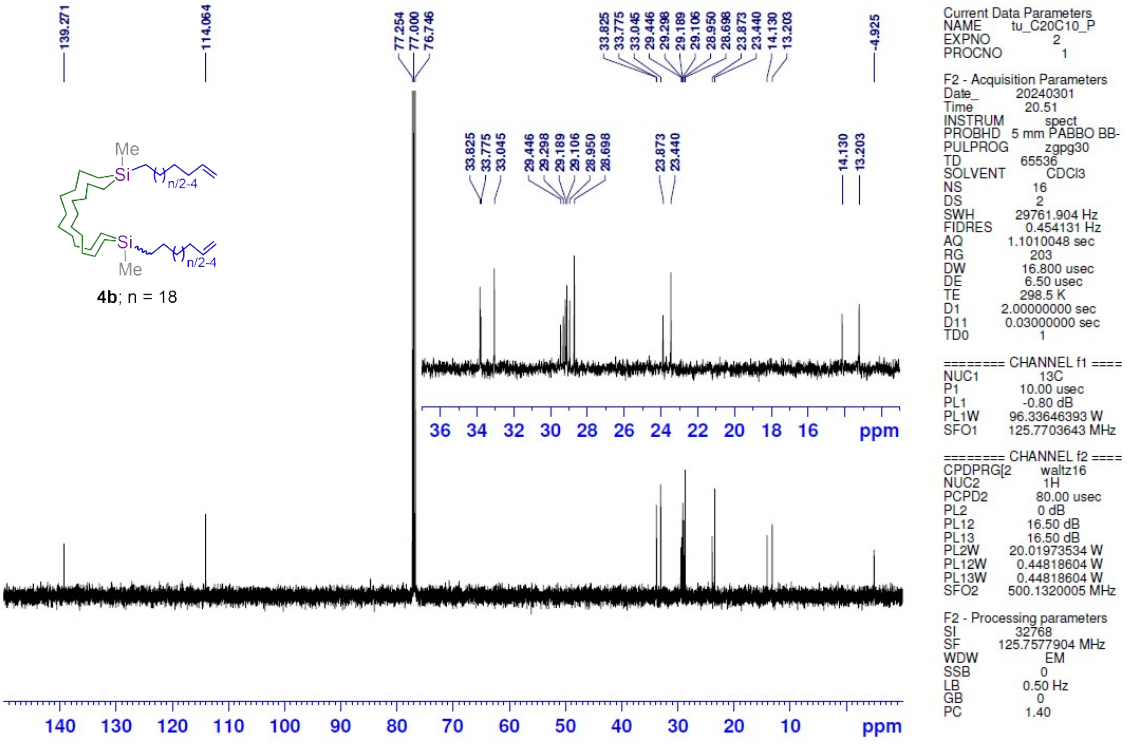

Fig. S24. ^{13}C NMR spectrum of **4b** in $CDCl_3$.

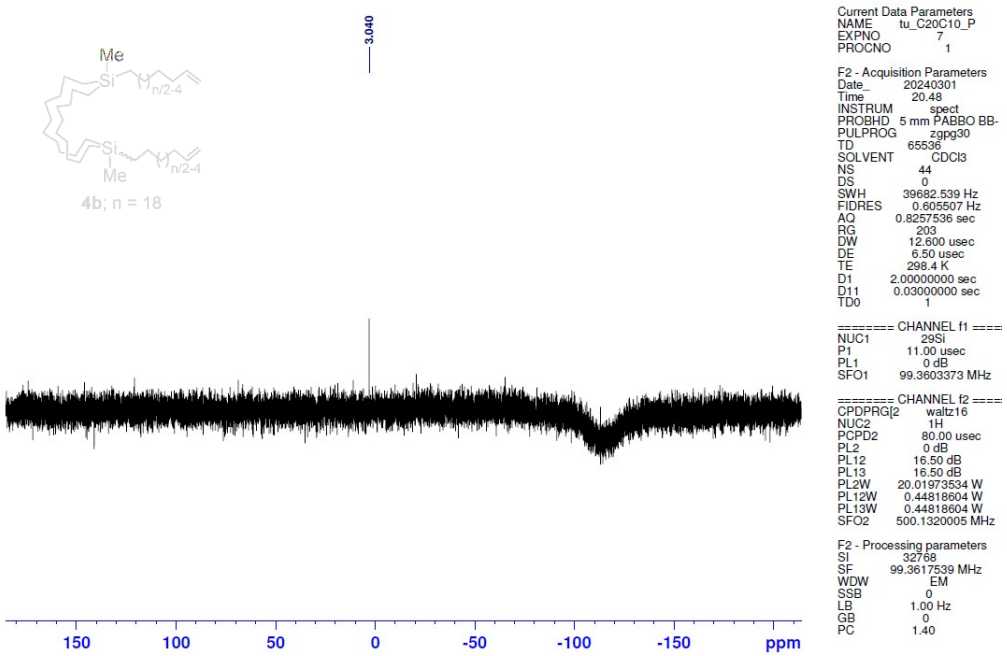

Fig. S25. ^{29}Si NMR spectrum of **4b** in $CDCl_3$.

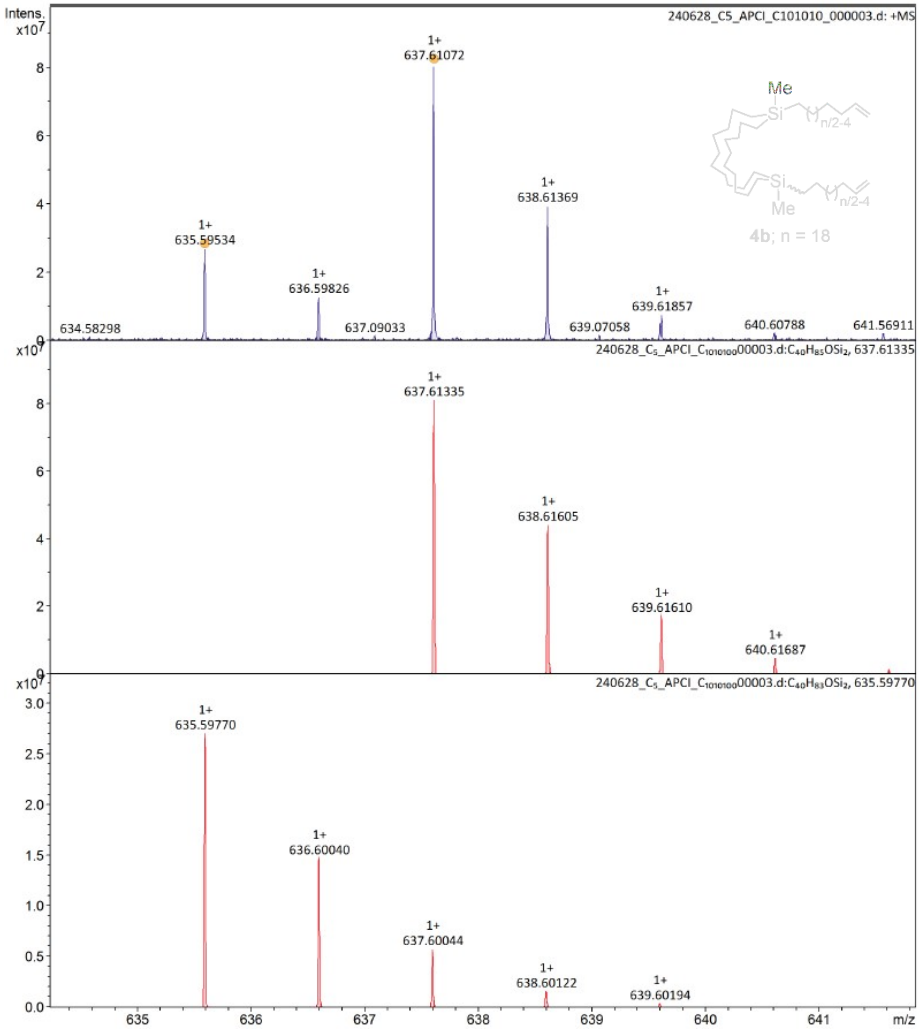

Fig. S26. HRMS spectrum of **4b** (APCI, positive). Top: obsd. Center and Bottom: sim.

3. Details of Temperature-Dependent NMR Study

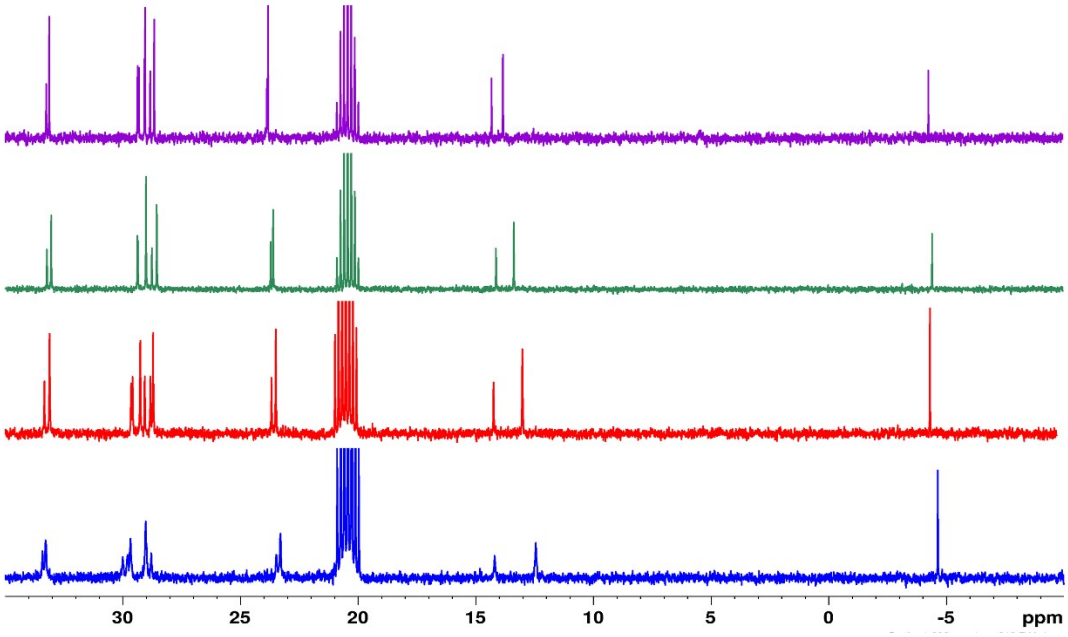

Fig. S27. Temperature-dependent ^{13}C NMR spectra of syn-**1b** in toluene-d_8: 300 K, 270 K, 240 K, and 210 K (top to bottom).

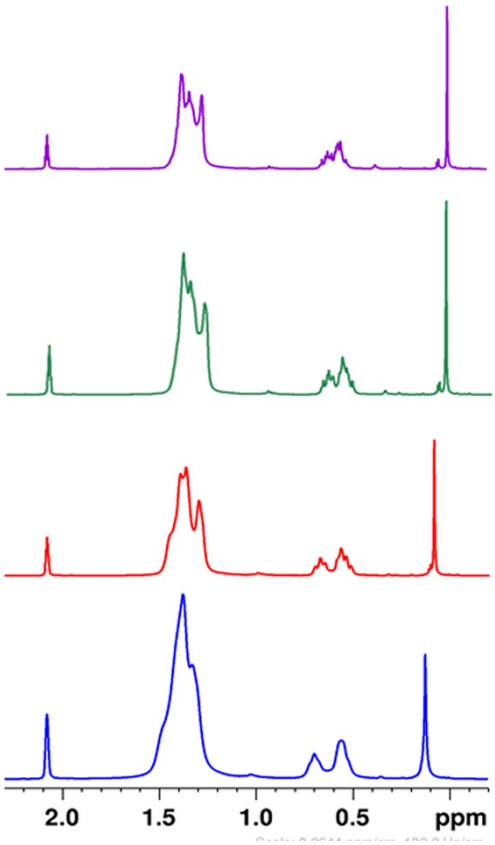

Fig. S28. Temperature-dependent ^{1}H NMR spectra of syn-**1b** in toluene-d_8: 300 K, 270 K, 240 K, and 210 K (top to bottom).

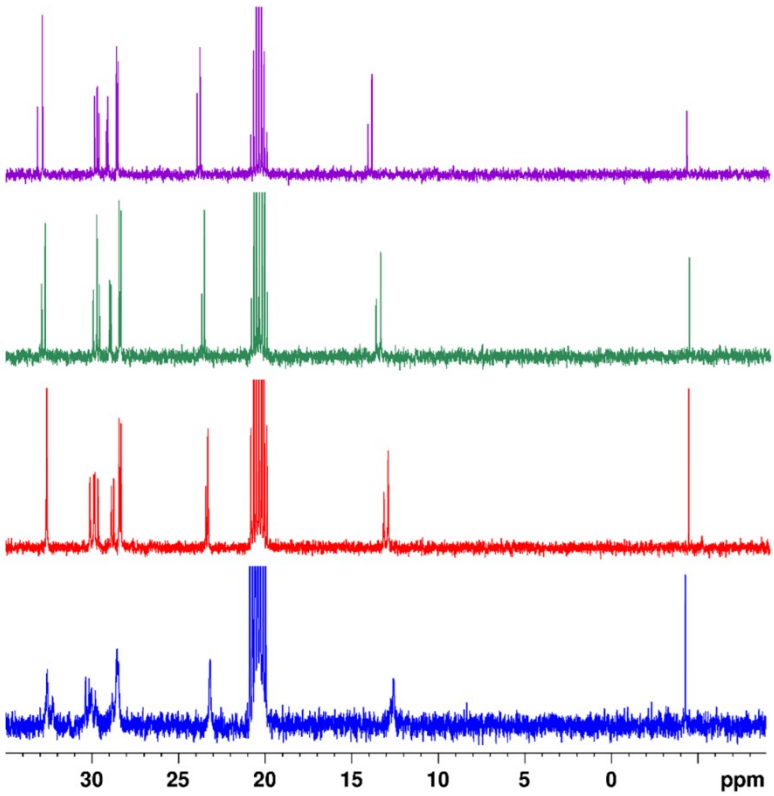

Fig. S29. Temperature-dependent ^{13}C NMR spectra of anti-**1b** in toluene-d_8: 300 K, 270 K, 240 K, and 210 K (top to bottom).

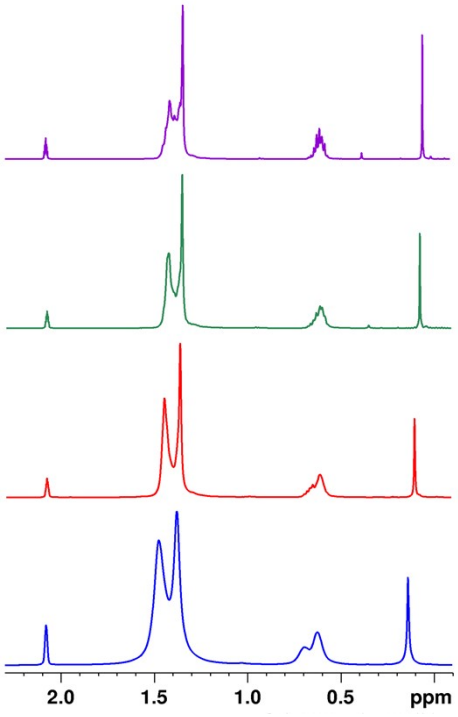

Fig. S30. Temperature-dependent ^{1}H NMR spectra of anti-**1b** in toluene-d_8: 300 K, 270 K, 240 K, and 210 K (top to bottom).

4. Details of X-ray Crystallography

Single-crystal X-ray crystallographic analyses were performed using a Bruker Venture diffractometer.

Table S1. Crystal Data

Compound		**2a**	**2b**	**trans-3**
CCDC #		2367922	2367923	2369099
Temperature		250(2) K	200(2) K	150 K
Empirical formula		C64 H132 Si4	C80 H164 Si4	C22 H46 F2 Si2
Crystal shape		prism	plate	prism
Crystal color		colorless	colorless	colorless
Crystal size		0.240 x 0.150 x 0.120 mm^3	0.160 x 0.140 x 0.060 mm^3	0.940 x 0.220 x 0.150 mm^3
Formula weight / g mol^{-1}		1014.05	1238.46	404.77
Crystal system		Triclinic	Orthorhombic	Triclinic
Space group		*P*−1	*Pbca*	*P*−1
Z		1	4	1
Calculated density		0.978 Mg/m^3	0.974 Mg/m^3	1.037 Mg/m^3
Cell parameter	*a*	10.0201(10) Å	14.9494(4) Å	5.8392(2) Å
	b	13.7449(13) Å	8.4932(2) Å	10.0661(3) Å
	c	13.8357(13) Å	66.5433(18) Å	11.6107(4) Å
	α	114.915(6)°	90°	88.9020(10)°
	β	92.110(5)°	90°	75.5770(10)°
	γ	92.923(5)°	90°	78.9050(10)°
	V	1722.4(3) $Å^3$	8448.9(4) $Å^3$	648.29(4) $Å^3$
F(000)		572	2800	224
Absorption coefficient		1.029 mm^{-1}	0.908 mm^{-1}	1.380 mm^{-1}
***θ* range for collection (deg)**		3.802 to 73.085° (Cu)	2.656 to 73.028° (Cu)	3.933 to 72.298° (Cu)
Index ranges		-12<=h<=12, -16<=k<=16, -16<=l<=17	-18<=h<=18, -9<=k<=10, -81<=l<=82	-6<=h<=7, -12<=k<=12, -14<=l<=14
Reflections collected		32186	121616	9532
Independent reflections		6601 [R(int) = 0.0579]	8371 [R(int) = 0.1447]	2462 [R(int) = 0.0301]
Completeness		97.5 %	99.6 %	96.6 %
Goodness-of-fit on F^2		1.041	1.049	1.075
Final R indices [I>2sigma(I)]		R1 = 0.0731, wR2 = 0.1837	R1 = 0.0672, wR2 = 0.1598	R1 = 0.0429, wR2 = 0.1275
R indices (all data)		R1 = 0.1002, wR2 = 0.2109	R1 = 0.0938, wR2 = 0.1759	R1 = 0.0433, wR2 = 0.1279
Largest diff. peak and hole		0.658 and -0.339 e.$Å^{-3}$	0.242 and -0.255 e.$Å^{-3}$	0.279 and -0.182 e.$Å^{-3}$

(a)

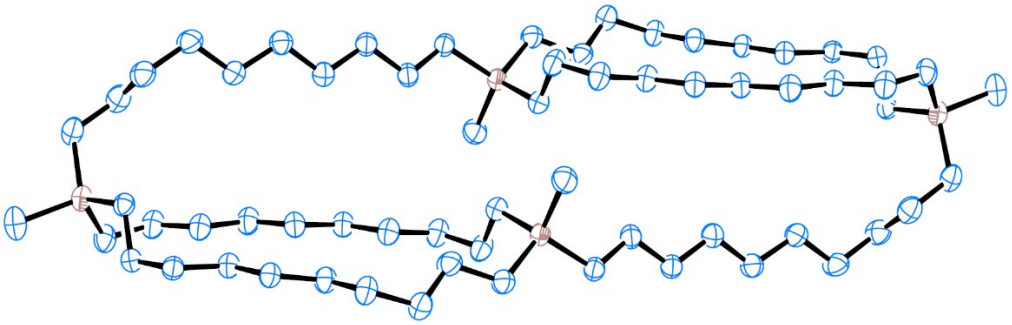

(b)

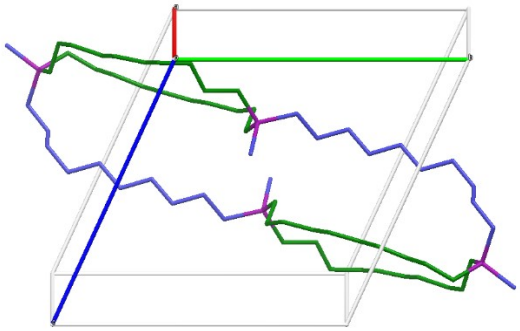

Fig. S31. (a) An ORTEP drawing (30% thermal ellipsoids) of molecular structure and (b) crystal packing structure of **2a** determined by X-ray crystallography.

(a)

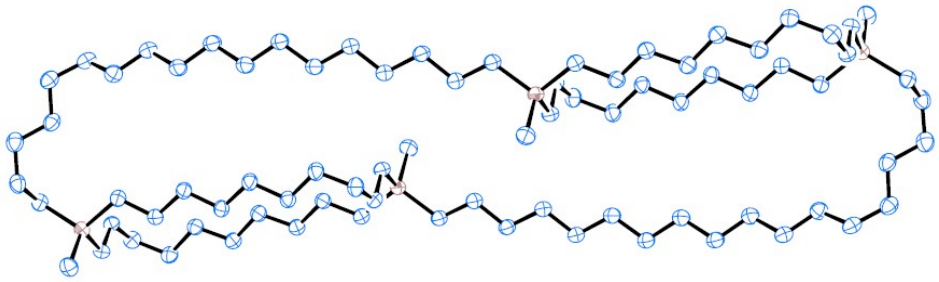

(b)

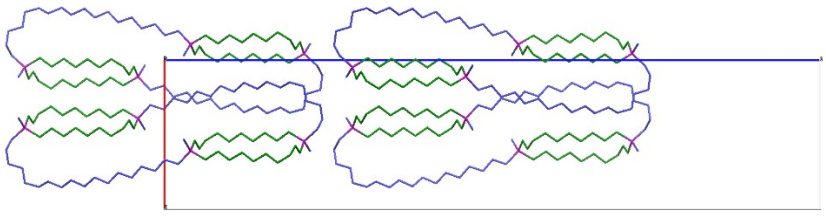

Fig. S32. (a) An ORTEP drawing (30% thermal ellipsoids) of molecular structure and (b) crystal packing structure of **2a** determined by X-ray crystallography.

(a)

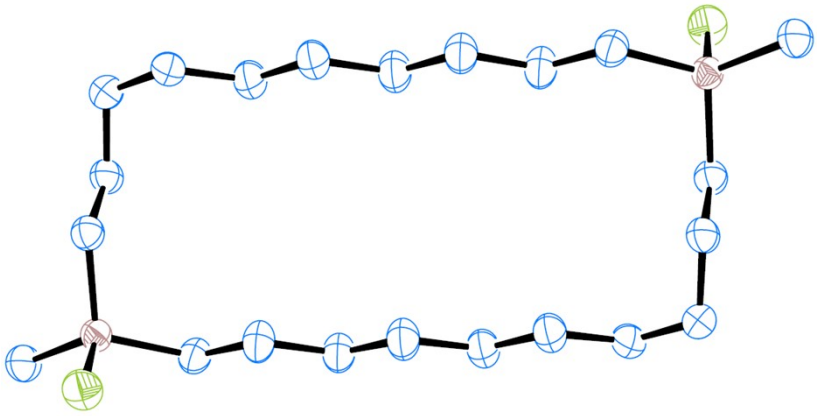

(b)

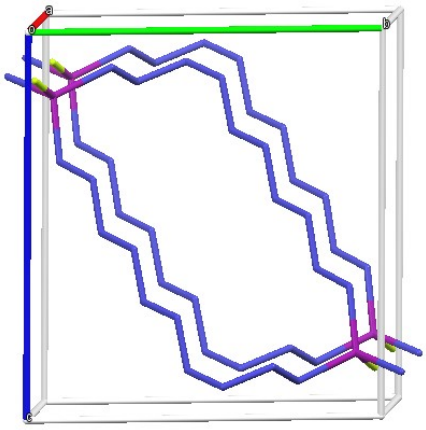

Fig. S33. (a) An ORTEP drawing (30% thermal ellipsoids) of molecular structure and (b) crystal packing structure of **trans-3** determined by X-ray crystallography.